


Optomagnonic Josephson effect in antiferromagnetsKouki Nakata *Advanced Science Research Center, Japan Atomic Energy Agency, Tokai, Ibaraki 319-1195, Japan*

(Received 2 May 2021; revised 1 August 2021; accepted 23 August 2021; published 1 September 2021)

Combining advanced technologies of optics and antiferromagnetic spintronics, we present a method to realize ultrafast spin transport. The optical Barnett effect provokes quasiequilibrium Bose-Einstein condensates (BECs) of magnons associated with the fully spin-polarized state in insulating antiferromagnets (AFs). This optomagnonic Barnett effect enables us to exploit coherent magnons of high frequency over the conventional ones of (sub-) terahertz associated with the Néel magnetic order. We show that the macroscopic coherence of those optical magnon BECs induces a spin current across the junction interface of weakly coupled two insulating AFs, and this optomagnonic Josephson effect realizes ultrafast spin transport. The period of the optomagnonic Josephson oscillation is much shorter than the conventional one of the order of picoseconds. Thus we propose a way to realize ultrafast spin transport in AFs by means of the macroscopic coherence of optical magnon BECs.

DOI: [10.1103/PhysRevB.104.104402](https://doi.org/10.1103/PhysRevB.104.104402)**I. INTRODUCTION**

For the realization of rapid and efficient transmission of information over electronics, inventing methods to handle a fast and flexible manipulation of spin transport is a central task in the field of spintronics [1–7]. For this goal, antiferromagnets (AFs) [8–16] have an advantage over ferromagnets (FMs) [17–20] in that spin dynamics is much faster. The energy scale of FMs is characterized by the macroscopic and classical magnetic dipole interaction in gigahertz (GHz) regime [17], and hence the spin Josephson oscillation [21] operates of the order of nanoseconds (ns) [4,22]. On the other hand, the energy scale of AFs arises from microscopic and quantum-mechanical spin exchange interactions. Therefore AFs can operate at much higher frequency. Thus AFs are expected to be the best platform for ultrafast transport of spin information [3,5,8–10]. The observation of spin currents by means of sub-terahertz (sub-THz) spin pumping in AFs was reported in Refs. [13,14]. Making use of the property of AFs, spin Josephson effects of THz associated with the Néel magnetic order [23] were theoretically proposed in Refs. [24,25]. The spin Josephson oscillation operates of the order of picoseconds (ps).

Another significant development in the manipulation of magnetism is the utilization of laser-matter coupling [26–29]. By means of the optical method [30–36], the reversal of magnetization was achieved experimentally [37–40], and an optical analog of the conventional Barnett effect [41–43], i.e., laser-induced magnetization [44,45], was proposed theoretically [35,36]. This optical Barnett effect even provokes quasiequilibrium Bose-Einstein condensates (BECs) of magnons [46], i.e., optical magnon BECs, and this behavior is especially called the optomagnonic Barnett effect [47]. Thus the interdisciplinary field between optics and magnonics [11,48–50], dubbed optomagnonics, has been attracting much attention.

In this paper, using the macroscopic coherence of the optical magnon BECs, we propose a method for the realization of ultrafast spin transport in insulating AFs. The optical Barnett effect realizes the fully spin-polarized state of insulating AFs. This enables us to exploit coherent magnons of high frequency over the conventional ones of (sub-) THz associated with the Néel magnetic order. We show that the macroscopic coherence of the optical magnon BECs induces a spin current across the junction interface of weakly coupled two insulating AFs (Fig. 1). We refer to this phenomenon as the optomagnonic Josephson effect. The period of the optomagnonic Josephson oscillation is much shorter than the conventional one of the order of picoseconds. This ultrafast phenomenon intrinsic to AFs, the optomagnonic Josephson effect, is the result from the confluence of optics and antiferromagnetic magnonics. We also discuss an experimental scheme for the observation.

We remark that in this paper using the scheme of Refs. [44,45], we consider transport of the optical magnon BECs in AFs, i.e., magnon BECs out of equilibrium, associated with the fully spin-polarized state of high frequency over the conventional one of (sub-) THz associated with the Néel magnetic order [51] (cf. Sec. III A). See Refs. [52,53] for magnon BECs in equilibrium subjected to a static magnetic field.

This paper is organized as follows. In Sec. II we quickly review the optical Barnett effect. Then we investigate the prominent application, the optomagnonic Josephson effect, in Sec. III and give an estimate for the experimental feasibility in Sec. IV. Finally, we remark on several issues in Sec. V and summarize in Sec. VI. Technical details are described in the Appendices.

II. OPTICAL BARNETT EFFECT

Before going to the main subject, for readers' convenience let us quickly review the mechanism of the laser-induced

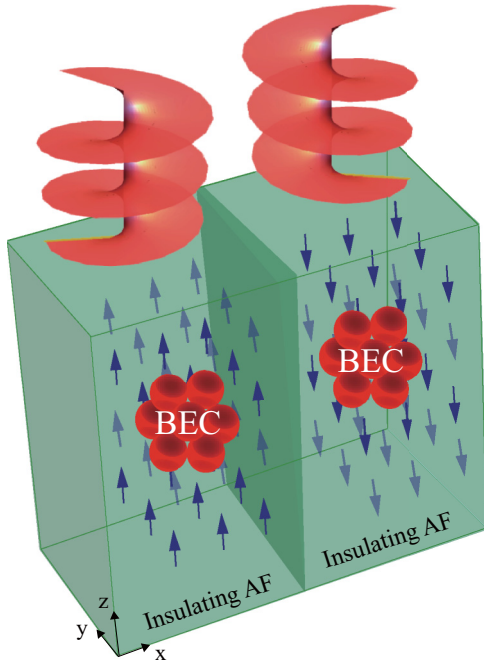


FIG. 1. Schematic picture of the optomagnonic Josephson junction. The two insulating AFs are separated by a thin film of a nonmagnetic insulator and weakly exchange coupled. We assume an identical material for each AF subjected to a circularly polarized laser with the opposite polarization $\eta = \pm$. In the vicinity of $\Omega = \Omega_{\text{BEC}}$, the optical Barnett effect realizes the quasiequilibrium magnon BEC, i.e., the optical magnon BEC, associated with the fully spin-polarized state in the high frequency regime, where spins in the left (right) AF are along the $+$ ($-$) z axis due to the opposite circular polarization (cf. Tables I and II).

magnetization [44,45], i.e., the optical Barnett effect [35,36]. See Refs. [44,45] for details [54], especially for the importance of modulating laser frequency adiabatically by the chirping technique [55,56].

We consider a magnetic insulator with a large electronic gap described by the Hamiltonian \mathcal{H}_0 which has the $U(1)$ symmetry about an axis, and we take the z axis for convenience. Due to the large electronic gap, spins in the circularly polarized laser interact only with the magnetic component of the laser through the Zeeman coupling. We take the polarization plane of the laser as the xy plane. We adiabatically apply the laser of the frequency $\Omega > 0$ with the magnetic field amplitude $B_0 > 0$. For the generation of the optical Barnett effect, the driving field amplitude $B_0 > 0$ should take a nonzero value $B_0 \neq 0$ of being strong enough that $B_0 > |u_0|$, where u_0 is the potential energy of magnons in the lattice formed by surroundings (e.g., phonons and impurities, etc.). Since throughout this paper we assume the clean magnet at low temperatures, the condition is satisfied. The spin system subjected to the laser is described by the time-periodic Hamiltonian $\hat{\mathcal{H}}(t) = \hat{\mathcal{H}}_0 - B_0[\hat{S}_{\text{tot}}^x \cos(\Omega t) + \eta \hat{S}_{\text{tot}}^y \sin(\Omega t)]$, where the sign $\eta = +(-)$ represents the left (right) circular polarization and $S_{\text{tot}}^{x(y,z)} := \sum_j S_j^{x(y,z)}$ is the summation over spin operators on all the spin sites. Using the unitary transformation, we obtain an effective static Hamiltonian in the rotational frame [57] of

the frequency $\eta\Omega$ around the z axis as [44,45]

$$\hat{\mathcal{H}}_{\text{eff}} = \hat{\mathcal{H}}_0 - \eta \hbar \Omega \hat{S}_{\text{tot}}^z + O(B_0). \quad (1)$$

Hereafter we assume a weak laser field $B_0 \ll \hbar \Omega$ where the $B_0 S_{\text{tot}}^x$ term is negligibly small. In Eq. (1), the effective magnetic field Ω/γ with the gyromagnetic ratio γ may be regarded as an optical analog [35,36] of the conventional Barnett field [41–43] along the z axis. This optical Barnett field develops the total magnetization of magnets. The direction of the optical Barnett field is controllable by means of the change of the laser chirality $\eta = \pm$. The effective static Hamiltonian $\hat{\mathcal{H}}_{\text{eff}}$ [Eq. (1)] has the $U(1)$ symmetry.

We remark that modulating laser frequency Ω slowly enough through the chirping technique [55,56], the adiabatic time evolution is realized [44,45]. Therefore the spin configuration is determined in the way that the energy of the Hamiltonian $\hat{\mathcal{H}}_{\text{eff}}$ [Eq. (1)] per site is minimized.

III. OPTOMAGNONIC JOSEPHSON EFFECT

A. Optical magnon BEC in AF

We apply the optical Barnett effect [Eq. (1)] to an insulating AF described by the Hamiltonian

$$\hat{\mathcal{H}}_0 = J \sum_{\langle i,j \rangle} \hat{S}_i \cdot \hat{S}_j + D \sum_i (\hat{S}_i^z)^2, \quad (2)$$

where $\hat{S}_{i(j)} = (\hat{S}_{i(j)}^x, \hat{S}_{i(j)}^y, \hat{S}_{i(j)}^z)$ represents the spin operator on the $i(j)$ th site having the spin quantum number S , $J > 0$ is the exchange interaction between the nearest neighbor spins $\langle i, j \rangle$, and $D > 0$ is the easy-plane single ion anisotropy that stabilizes the Néel magnetic order on the xy plane. Hereafter, we consider a cubic lattice.

First, the optical Barnett field [Eq. (1)] develops the total magnetization of the AF along the z axis continuously. We find from a microscopic calculation [51] that in the high frequency regime $\Omega > \Omega_{\text{BEC}}$ defined as

$$\Omega_{\text{BEC}} := 2(6J + D)S/\hbar \quad (3)$$

spins are fully polarized along the ηz axis, and confirmed the absence of the first order transition in the vicinity of Ω_{BEC} [51]. This assures the validity of the description in terms of the magnon picture [58]. Hence we move to the analysis by the magnon theory next. For the details of the calculation, see the Appendices [51].

Note that magnons acquire the effective magnetic field in the corotating frame as [51] $\mathbf{B}_{\text{eff}} = (B_{\text{eff}}^x, 0, B_{\text{eff}}^z)$, where $B_{\text{eff}}^x := B_0$ along the x axis and $B_{\text{eff}}^z := \hbar(\Omega - \Omega_{\text{BEC}}) + 6JS$ along the z axis. Since $6JS \gg B_0$ in general, the effective magnetic field along the x axis $B_{\text{eff}}^x = B_0$ is negligibly small compared with the z component $B_{\text{eff}}^z \ll B_{\text{eff}}^z$ even in the vicinity of $\Omega \approx \Omega_{\text{BEC}}$. Throughout this paper we work under the assumption that $0 < |u_0| < B_0 \ll \hbar \Omega, 6JS$.

Next, decreasing the frequency Ω from above the critical value Ω_{BEC} in which spins are full polarized, magnon BEC transition is provoked on the point $\Omega = \Omega_{\text{BEC}}$ and magnons of π mode, $\mathbf{k} = \boldsymbol{\pi} := (\pi/a, \pi/a, \pi/a)$, begin to condensate, where \mathbf{k} is the wave number and a is the lattice constant. We refer to this behavior as the optomagnonic Barnett effect, and the resulting magnon condensate as the optical magnon

TABLE I. Comparison of the optical magnon BECs in the junction of AFs shown in Fig. 1.

	Left BEC	Right BEC
Frequency	$O(10)$ THz	$O(10)$ THz
Circular polarization	$\eta = +$	$\eta = -$
Spin polarization	$+z$ axis	$-z$ axis
Spin angular momentum	$-$	$+$
Macroscopic coherent state	$b_L = \sqrt{N_L} e^{i\theta_L}$	$b_R = \sqrt{N_R} e^{-i\theta_R}$

BEC [47]. In the frequency $\Omega < \Omega_{\text{BEC}}$, the AF acquires a transverse component of local magnetization associated with the spontaneous $U(1)$ symmetry breaking, and thus forms a macroscopic coherent state. The optical magnon BEC state is described by the effective Hamiltonian in the rotational frame of the frequency $\eta\Omega$ around the z axis as [51]

$$\hat{\mathcal{H}}_{\text{eff}}(\mathbf{k} = \boldsymbol{\pi}) = \hbar(\Omega - \Omega_{\text{BEC}})\hat{a}_{\boldsymbol{\pi}}^\dagger\hat{a}_{\boldsymbol{\pi}} + U\hat{a}_{\boldsymbol{\pi}}^\dagger\hat{a}_{\boldsymbol{\pi}}^\dagger\hat{a}_{\boldsymbol{\pi}}\hat{a}_{\boldsymbol{\pi}}, \quad (4)$$

where $\hat{a}_{\boldsymbol{\pi}}^{(\dagger)}$ is the bosonic annihilation (creation) operator for magnons of the π mode in condensation,

$$U := \frac{\hbar\Omega_{\text{BEC}}}{2SN} \quad (5)$$

represents the magnitude of magnon-magnon interactions, and N is the number of spin sites. The magnon-magnon interaction is repulsive $U > 0$. Therefore the magnon BEC characterized by the expectation value $\langle\hat{a}_{\boldsymbol{\pi}}\rangle \neq 0$ are stable [52].

Finally, the effective Hamiltonian for the optical magnon BEC in the rotational frame is recast into the Hamiltonian in the original stationary reference frame as [51]

$$\hat{\mathcal{H}}_{k=\pi} = -\hbar\Omega_{\text{BEC}}\hat{b}_{\pi}^\dagger\hat{b}_{\pi} + U\hat{b}_{\pi}^\dagger\hat{b}_{\pi}^\dagger\hat{b}_{\pi}\hat{b}_{\pi}, \quad (6)$$

where $\hat{b}_{\pi}^{(\dagger)}$ is the magnon operator in the reference frame and $\hat{a}_{\mathbf{k}}^{(\dagger)} = \hat{R}^\dagger\hat{b}_{\mathbf{k}}^{(\dagger)}\hat{R}$ for $\hat{R} := \exp(\eta i\Omega t \hat{S}_{\text{tot}}^z)$. This Hamiltonian depends solely on the material parameters Ω_{BEC} [Eqs. (3) and (5)], while it is independent of laser frequency. Note that the number of magnon BECs is characterized as a function of laser frequency [51].

We remark that condensation of the π mode magnons does not induce a Josephson-like effect in the single AF since the xy components of the nearest neighbor spins are in the opposite direction and this results in $\sin(\pm\pi) = 0$.

B. Optomagnonic Josephson junction

In this paper, using the optical magnon BEC in the vicinity of $\Omega = \Omega_{\text{BEC}}$, we investigate the application of the macroscopic coherence to ultrafast spin transport. To this end, we consider a junction of weakly exchange-coupled two insulating AFs shown in Fig. 1. The two AFs are separated by a thin film of a nonmagnetic insulator [24] and weakly exchange coupled. The AFs are subjected to a circularly polarized laser of the frequency $\Omega < \Omega_{\text{BEC}}$ with the opposite polarization $\eta = \pm$. Thus optical magnon BECs are realized and spins of the left (right) AF are aligned along the $+$ ($-$) z axis due to the opposite circular polarization (Table I).

First, we assume an identical material for each AF. From Eq. (6) the optical magnon BEC in the left (right) AF is

described by the Hamiltonian $\hat{\mathcal{H}}_{L(R)}$ in the original stationary frame as [51]

$$\hat{\mathcal{H}}_L = \hbar\Omega_L\hat{b}_L^\dagger\hat{b}_L + U_L\hat{b}_L^\dagger\hat{b}_L^\dagger\hat{b}_L\hat{b}_L, \quad (7a)$$

$$\hat{\mathcal{H}}_R = \hbar\Omega_R\hat{b}_R^\dagger\hat{b}_R + U_R\hat{b}_R^\dagger\hat{b}_R^\dagger\hat{b}_R\hat{b}_R, \quad (7b)$$

where

$$\Omega_L = \Omega_R := -\Omega_{\text{BEC}} < 0, \quad (8a)$$

$$U_L = U_R := U > 0, \quad (8b)$$

and $\hat{b}_{L(R)}^{(\dagger)}$ is the bosonic annihilation (creation) operator for magnon condensates of the π mode in the left (right) AF.

Next, we focus on the junction interface connecting the two AFs. Due to a finite overlap of the wave functions of the localized spins that reside on the relevant two-dimensional boundaries of each insulator, there exists in general a finite exchange interaction between the boundary spins [22,59]. This induces a tunneling process of magnons across the junction interface. Let us denote the tunneling amplitude as $|K|$. Since two AFs are separated by a thin film of a nonmagnetic insulator [24], those are weakly exchange coupled. In the tunneling limit the energy scale is assumed to be $|K| \ll |\hbar\Omega_{L(R)}|$ and $|K| \ll J$. During the tunneling process, the spin angular momentum is exchanged between the left and the right BECs via magnons. Since spins in the left (right) AF are aligned along the $+$ ($-$) z axis by the opposite circular polarization $\eta = \pm$, the magnon of the left BEC carries the spin angular momentum $\delta S_L^z = -$, while that of the right BEC carries the opposite $\delta S_R^z = +$. Therefore, within the low energy regime (i.e., in the lowest order of magnon operators), from the conservation law of the total spin angular momentum, the tunneling process at the junction interface is effectively described by the Hamiltonian [51] $\hat{V} = -K(\hat{b}_L\hat{b}_R + \hat{b}_L^\dagger\hat{b}_R^\dagger)$, where $\text{sgn}(K) = \pm$ in general [24,60]. Note that the total number of magnons is not conserved due to this tunneling process.

Finally, the total Hamiltonian for the optomagnonic Josephson junction, Fig. 1, is summarized as $\hat{\mathcal{H}}_{\text{tot}} = \hat{\mathcal{H}}_L + \hat{\mathcal{H}}_R + \hat{V}$. See the Appendices for the tunneling amplitude in spin language [51].

C. Optomagnonic Josephson equation

Starting from the Hamiltonian $\hat{\mathcal{H}}_{\text{tot}}$ of the junction system, we derive the spin Josephson equation of the optomagnonic Barnett effect. First, since the optical magnon BEC is a macroscopic coherent state, it acquires a macroscopic coherence $\langle\hat{b}_{L(R)}(t)\rangle =: b_{L(R)}(t) \neq 0$ characterized as $b_L(t) = \sqrt{N_L(t)} e^{i\theta_L(t)} \in \mathbb{C}$ and $b_R(t) = \sqrt{N_R(t)} e^{-i\theta_R(t)} \in \mathbb{C}$, where $N_{L(R)}(t)$ is the number of magnon BECs in the left (right) insulator and $\theta_{L(R)}$ is the phase [4]. The sign change in the phase, $i\theta_L(t)$ and $-i\theta_R(t)$, arises from the fact that spins of the left (right) AF are aligned along the $+$ ($-$) z axis by the opposite circular polarization $\eta = \pm$; the spin raising operation corresponds to the magnon annihilation in the left BEC, while to the magnon creation in the right BEC (Table I).

Next, using the Heisenberg equation of motion for $\hat{\mathcal{H}}_{\text{tot}}$ and taking the expectation value $\langle\hat{b}_{L(R)}(t)\rangle =: b_{L(R)}(t)$, we

derive [51] the two-state model [22,61] for the optical magnon BECs:

$$i\hbar \frac{db_L(t)}{dt} = \hbar\Omega_L b_L + 2U_L N_L b_L - K b_R^\dagger, \quad (9a)$$

$$i\hbar \frac{db_R(t)}{dt} = \hbar\Omega_R b_R + 2U_R N_R b_R - K b_L^\dagger. \quad (9b)$$

Then we divide Eqs. (9a) and (9b) into the real and imaginary parts as

$$\frac{d}{dt}[N_L(t) - N_R(t)] = 0, \quad (10a)$$

$$\frac{d}{dt}[N_L(t) + N_R(t)] = -\frac{4K}{\hbar} \sqrt{N_L N_R} \sin(\theta_R - \theta_L), \quad (10b)$$

$$-\hbar \frac{d\theta_L(t)}{dt} = (\hbar\Omega_L + 2U_L N_L) - K \sqrt{\frac{N_R}{N_L}} \cos(\theta_R - \theta_L), \quad (10c)$$

$$\hbar \frac{d\theta_R(t)}{dt} = (\hbar\Omega_R + 2U_R N_R) - K \sqrt{\frac{N_L}{N_R}} \cos(\theta_R - \theta_L). \quad (10d)$$

Equations (10a) and (10b) mean that the total number of magnons in condensation $N_+(t) := N_L(t) + N_R(t)$ is not conserved due to the tunneling process, while the total spin angular momentum $N_- := N_L(t) - N_R(t)$ is conserved. This ensures that the left BEC acquires the spin angular momentum lost in the right BEC, and vice versa. The initial condition $N_+(0)$ and $N_-(0)$, i.e., $N_{L(R)}(0)$, is characterized as a function of laser frequency [51].

Finally, we introduce the variable $z(t)$ to describe the spin current across the junction interface as $z(t) := N_+(t)/N_-$, and define the relative phase as $\theta(t) := \theta_R(t) - \theta_L(t)$, where $|z(t)| \geq 1$ by definition. In this work, without loss of generality, we assume the initial condition $N_-(0) > 0$ for convenience. Since $N_- := N_L - N_R$ is constant, this ensures $z(t) \geq 1$. In terms of the variables $z(t)$ and $\theta(t)$, Eqs. (10a)–(10d) are summarized as [51]

$$\frac{dz(t)}{dt} = -\frac{2K}{\hbar} \sqrt{z(t)^2 - 1} \sin\theta(t), \quad (11a)$$

$$\frac{d\theta(t)}{dt} = \left[(\Omega_L + \Omega_R) + \frac{U_L - U_R}{\hbar} N_- \right] + \left(\frac{U_L + U_R}{\hbar} N_- \right) z(t) - \frac{2K}{\hbar} \frac{z(t)}{\sqrt{z(t)^2 - 1}} \cos\theta(t). \quad (11b)$$

This is the spin Josephson equation for the junction of the AFs shown in Fig. 1 subjected to the optomagnonic Barnett effect. We refer to this equation as the optomagnonic Josephson equation. Equation (11a), $dz(t)/(dt) \propto \sin\theta(t)$, describes the Josephson spin current across the junction interface, and Eq. (11b), $d\theta/(dt)$, shows the time evolution of the relative phase. The numerical plot of the Josephson spin current is depicted in Fig. 2. Equation (11a) means that due to the macroscopic coherence of the optical magnon BEC, the spin current of $O(K)$ arises from the phase difference. This is in contrast to the junction of noncondensed magnons

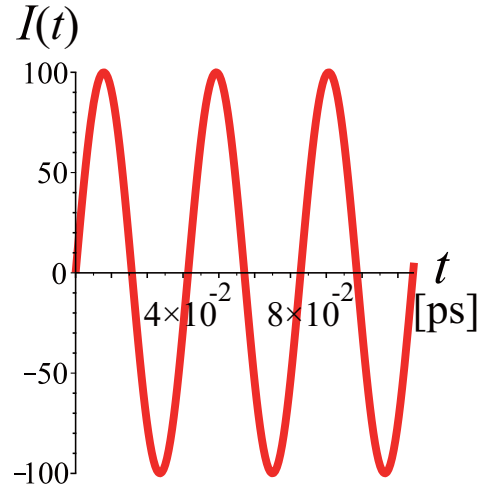


FIG. 2. Plot of the rescaled Josephson spin current $I(t) := [\hbar/(2K)][dz/(dt)]$ as a function of time in the vicinity of $\Omega = \Omega_{\text{BEC}} = 75$ THz obtained by numerically solving Eqs. (11a) and (11b) with the initial condition $z(0) = 10^2$ and $\theta(0) = 0$ for experimental values given in the main text. Assuming $K = 0.375 \mu\text{eV}$, the period of the optomagnonic Josephson oscillation becomes $O(10^{-2})$ ps.

[59], where spin currents of $O(K^2)$ are generated, e.g., by the temperature difference. Note that being independent of the sign of the parameter K , the spin Josephson effect is induced; Eqs. (11a) and (11b) are invariant under the transformation $K \rightarrow -K$ and $\theta(t) \rightarrow \theta(t) + \pi$. Thus the effect of the sign change $\text{sgn}(K) = \pm$ is absorbed into the initial condition of the relative phase and the transport property remains unchanged essentially.

We remark that the quasiequilibrium magnon BEC of π mode corresponds to a macroscopic coherent spin precession where the xy components of the nearest neighbor spins in the single AF are in the opposite direction. This does not affect the Josephson effect in the junction of the AFs since the Josephson equations [Eqs. (11a) and (11b)] are invariant under the transformation $\theta(t) \rightarrow \theta(t) + 2\pi$.

D. Optomagnonic Josephson spin current

The transition point for the optical magnon BEC of the AF amounts to $\Omega_{\text{BEC}} = O(10)$ THz. Under some conditions, Eq. (11b) approximately reduces to $d\theta(t)/(dt) \approx \Omega_L + \Omega_R$ and essentially results in $\theta(t) = (\Omega_L + \Omega_R)t + \theta(0)$. From Eq. (11a) we find that $dz(t)/(dt) \propto \sin[(\Omega_L + \Omega_R)t + \theta(0)]$. The period of the optomagnonic Josephson oscillation is estimated to be $2\pi/|\Omega_L + \Omega_R| = O(10^{-2})$ ps. Thus ultrafast spin transport is realized in AFs. We refer to this phenomenon as the optomagnonic Josephson effect. The analytic estimation agrees with the numerical calculation shown in Fig. 2.

IV. EXPERIMENTAL FEASIBILITY

For an estimate we assume the following experiment parameter values for an insulating AF, NiO, as [62–64] $J = 6.3$ meV, $D = 0.1$ meV, and $S = 1$. We find that the transition point for the optical magnon BEC amounts to

TABLE II. The comparison of the spin Josephson effect in the AF-AF junction; the conventional spin Josephson effect of Refs. [24,25] and the optomagnonic Josephson effect of this study (Fig. 1).

	Conventional	Optomagnonic
Order	Néel magnetic order	Fully spin-polarized state
Coherence	e.g., AF resonance	Optical Barnett effect
Frequency	Sub-THz or $O(1)$ THz	$O(10)$ THz
Period	$O(1)$ ps	$O(10^{-2})$ ps

$\Omega_{\text{BEC}} = 75$ THz, which is much higher than the conventional one $\Omega_{\text{res}} = O(1)$ THz or sub-THz for the antiferromagnetic resonance associated with the Néel magnetic order [13,14,24,25]. The numerical plot of the optomagnonic Josephson effect is in Fig. 2 with the parameter values in its caption. Given these estimates we expect that, while being challenging, our proposal will be within experimental reach with current device and measurement technologies, e.g., femtosecond mid-infrared pump-probe spectroscopy [30,65–68] for the ultrafast spin dynamics, and Brillouin light scattering (BLS) [17,69] for the optical magnon BEC and the resulting Josephson effect. Reference [70] reported the observation of the AC Josephson effect of magnon BECs in $^3\text{He-B}$. We expect from a theoretical viewpoint that to use the inverse spin Hall effect [71] by attaching a metal to the insulating AF will be one of the most promising strategies for the observation of the magnon Josephson effect in magnets.

V. DISCUSSION

We remark on the difference between this study and other works on spin Josephson effects proposed in Refs. [22,24,25]. In the conventional low frequency region of the AF, coherent magnons associated with the Néel magnetic order are available, e.g., by antiferromagnetic resonance [15]. However, the frequency of the conventional coherent magnons can amount only to $\Omega_{\text{res}} = O(1)$ THz or sub-THz [13,14]. Thus the period of the resulting Josephson-like effect is estimated to be $O(1)$ ps [24,25]. Note that the quasiequilibrium magnon BEC of Ref. [22] through microwave pumping in FMs is in the $O(1)$ GHz regime [17], in much lower frequency, where the spin Josephson oscillation operates of the order of ns.

There is a distinction also in the spin Josephson equation due to the direction of the macroscopic coherent spin precession in the BEC phase. In the same way as in Ref. [22], the Josephson spin current of this work [Eqs. (11a) and (11b)] is proportional to $\sin\theta(t)$. However, in contrast to Ref. [22], the relative phase of this work is described essentially as the sum of the frequency $\Omega_{L(R)}$ of the left (right) BEC as $\theta(t) = \theta_R(t) - \theta_L(t) = (\Omega_L + \Omega_R)t + \theta(0)$ where $\text{sgn}(\Omega_L) = \text{sgn}(\Omega_R)$ [Eq. (8a)]. This arises from that through the optomagnonic Barnett effect of the opposite circular polarization $\eta = \pm$, spins in the left (right) AF are aligned along the $+$ ($-$) z axis, see Fig. 1 (cf. Table I). Consequently, the direction of the macroscopic coherent spin precession in the left BEC phase becomes opposite to the one in the right. Therefore the relative phase becomes the sum of the frequency as $\theta(t) = (\Omega_L + \Omega_R)t + \theta(0)$ with $\text{sgn}(\Omega_L) = \text{sgn}(\Omega_R)$. On the

TABLE III. The comparison of the spin Josephson effect; the FM-FM junction of Ref. [22] through microwave pumping, and the AF-AF junction of this work (Fig. 1) through the optomagnonic Barnett effect, where $\text{sgn}(\omega_L) = \text{sgn}(\omega_R)$ and $\text{sgn}(\Omega_L) = \text{sgn}(\Omega_R)$, respectively. See Ref. [22] for the details of the frequency $\omega_{L(R)}$ of the left (right) BEC in the FM-FM junction.

	FM-FM junction	AF-AF junction
Magnon BEC	Microwave pumping	Optical Barnett
Total magnon number	Conserved	Nonconserved
Spin angular momentum	Conserved	Conserved
Josephson oscillation	$\sin[(\omega_L - \omega_R)t]$	$\sin[(\Omega_L + \Omega_R)t]$
Frequency	$O(1)$ GHz	$O(10)$ THz
Period	$O(1)$ ns	$O(10^{-2})$ ps

other hand, since spins in the FM-FM junction of Ref. [22] are aligned along the same direction, the relative phase is characterized essentially as the difference of the frequency $\omega_{L(R)}$ of the left (right) BEC as $(\omega_L - \omega_R)t$ where $\text{sgn}(\omega_L) = \text{sgn}(\omega_R)$. For the details of the frequency $\omega_{L(R)}$, see Ref. [22]. Thus, using the scheme of Fig. 1 we can enhance the frequency of the Josephson oscillation. For all of these reasons, ultrafast spin transport is realized in our AF-AF junction. Those are summarized in Tables II and III.

Several comments on our approach are in order. First, in this paper we assume not the easy-axis anisotropy but the easy-plane anisotropy. Therefore a spin-flop transition [72] is absent in this setup [51]. Second, we find that a DC spin Josephson effect might be induced but realized unstably in this setup [51]. Third, for the difference between the inverse Faraday effect [30,32] and the optical Barnett effect [35,36], i.e., the laser-induced magnetization [44,45], see Ref. [47]. Last, throughout this paper we have assumed a sufficiently low temperature where phonon degrees of freedom ceases to work [73–76]. It will be interesting to study the effect of phonons on the spin Josephson effect, which we leave for future work.

We remark that Ref. [77] reported experimental signatures of spin superfluid in Cr_2O_3 subjected to a strong magnetic field along the easy axis. For the generation of the spin superfluid [53], the easy-plane anisotropy is essential, while originally Cr_2O_3 possesses the easy-axis anisotropy. From this, it is expected that the applied magnetic field changes the spin anisotropy of Cr_2O_3 and effectively makes it the easy plane. Thus we can control the spin anisotropy. Still, to find the insulating AF which intrinsically possesses the perfect easy-plane anisotropy, i.e., the $U(1)$ spin-rotational symmetry within the easy plane, is of significance. To the best of our knowledge, this remains a challenge of the antiferromagnetic spintronics study.

VI. CONCLUSION

Using the macroscopic coherence of the optical magnon Bose-Einstein condensates intrinsic to insulating antiferromagnets, we have proposed the optomagnonic Josephson effect. The optomagnonic Barnett effect associated with the fully spin-polarized state enables us to exploit coherent magnons of high frequency over the conventional ones of (sub-) terahertz associated with the Néel magnetic order.

Applying the optomagnonic Barnett effect to the junction of weakly coupled two insulating antiferromagnets, we have shown that the ultrafast spin Josephson effect of those optical magnon Bose-Einstein condensates is realized. The period of the optomagnonic Josephson oscillation is much shorter than the conventional one of the order of picoseconds. Our work builds a bridge between optics and magnonics, and is expected to become the key ingredient for the ultrafast manipulation of spin information.

ACKNOWLEDGMENTS

The author would like to sincerely thank S. Takayoshi for fruitful discussions, especially for sharing his technical note; a part of the Appendices is based on it. The author is grateful also to K. A. van Hoogdalem, P. Simon, and D. Loss for the collaborative work on the related topic, Y. Korai for helpful discussions at the early stage of this work, S. K. Kim for useful information and comments on this manuscript, and M. Oka for helpful feedback on this work. The author is supported by JSPS KAKENHI Grant No. JP20K14420 and by Leading Initiative for Excellent Young Researchers, MEXT, Japan.

APPENDIX A: CLASSICAL SPIN THEORY

In this Appendix we derive the critical frequency Ω_c for the fully spin-polarized state of AFs, and evaluate the magnetization along the z axis as a function of laser frequency (Fig. 3). First, we consider the antiferromagnetic model described by

the Hamiltonian

$$\hat{\mathcal{H}}_0 = J \sum_{\langle i,j \rangle} \hat{\mathbf{S}}_i \cdot \hat{\mathbf{S}}_j + D \sum_i (\hat{S}_i^z)^2. \quad (\text{A1})$$

The easy-plane single ion anisotropy $D > 0$ stabilizes the Néel magnetic order on the xy plane. Under the application of circularly polarized laser, the effective Hamiltonian reduces to (see the main text)

$$\hat{\mathcal{H}}_{\text{eff}} = \hat{\mathcal{H}}_0 - \eta \hbar \Omega \sum_i \hat{S}_i^z. \quad (\text{A2})$$

The AF consists of the sublattice A and B. The classical spin configuration is determined in the way that the energy per spin ϵ ,

$$\epsilon = \frac{E}{N} \quad (\text{A3a})$$

$$= \frac{z_0 J}{2} \mathbf{S}_A \cdot \mathbf{S}_B + \frac{D}{2} [(S_A^z)^2 + (S_B^z)^2] - \frac{\eta \hbar \Omega}{2} (S_A^z + S_B^z) \quad (\text{A3b})$$

is minimized, where N is the number of spin sites, E denotes the total energy, z_0 represents the coordination number, and $\mathbf{S}_{A(B)}$ is the spin on the sublattice A (B).

Next, we focus on the vicinity of the critical frequency Ω_c (Fig. 3). Since Eq. (A3b) has the $U(1)$ symmetry, without loss of generality, we assume that \mathbf{S}_A and \mathbf{S}_B are in the xz plane as $\mathbf{S}_A = (S \sin \theta, 0, \eta S \cos \theta) =: (m_A^x, 0, m_A^z)$ and $\mathbf{S}_B = (-S \sin \theta, 0, \eta S \cos \theta) =: (m_B^x, 0, m_B^z)$. Then Eq. (A3b) is rewritten as

$$\epsilon = \frac{z_0 J S^2}{2} \cos(2\theta) + D S^2 \cos^2 \theta - \hbar \Omega S \cos \theta \quad (\text{A4a})$$

$$= (z_0 J + D) S^2 \cos^2 \theta - \hbar \Omega S \cos \theta - \frac{z_0 J S^2}{2}. \quad (\text{A4b})$$

We call the $0 < \theta < \pi$ case as the V-shape phase, which corresponds to the magnon BEC phase as we see below, since the sublattice magnetization \mathbf{S}_A and \mathbf{S}_B form the V shape. For the stability of the V-shape phase $0 < \theta < \pi$, the condition

$$z_0 J + D > 0 \quad (\text{A5})$$

is necessary. This condition corresponds to the repulsive interaction between magnons in the spin wave theory (cf. Appendix B). The energy of Eq. (A3b) takes the minimum at $\theta = 0$ for $\hbar \Omega \geq 2(z_0 J + D)S$ and at $\theta = \arccos\{\hbar \Omega / [2(z_0 J + D)S]\} \neq 0$ for $\hbar \Omega < 2(z_0 J + D)S$. Thus the critical frequency for the fully spin-polarized state of AFs is given as

$$\hbar \Omega_c = 2(z_0 J + D)S. \quad (\text{A6})$$

Finally, magnetization along the z axis per spin is given as

$$\eta S^z = S \cos \theta \quad (\text{A7a})$$

$$= \frac{\hbar \Omega}{2(z_0 J + D)} \quad (\text{A7b})$$

$$= \frac{\Omega}{\Omega_c} S. \quad (\text{A7c})$$

The numerical plot is provided in Fig. 3.

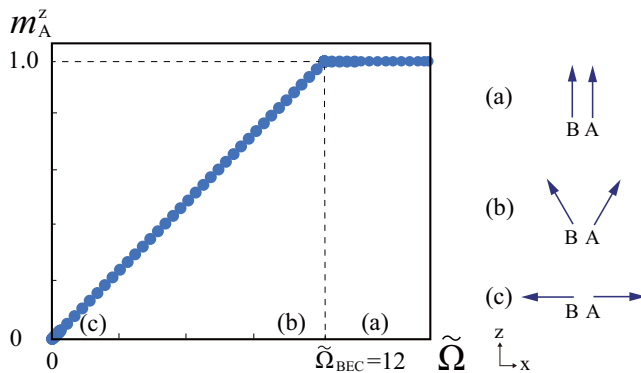


FIG. 3. Plot of the magnetization along the z axis $m_A^z = m_B^z$ for $\eta = 1$ as a function of the rescaled frequency $\tilde{\Omega} := \hbar \Omega / J$ obtained by numerically solving Eq. (A4b), i.e., minimizing the energy ϵ , with the experimental parameter values given in the main text. The optical Barnett field develops the magnetization continuously. The absence of the first order transition, i.e., jump of $m_{A(B)}^z$, assures the validity of the description in terms of magnons. (a) In the high frequency regime $\tilde{\Omega} > \tilde{\Omega}_{\text{BEC}} = 12$, spins are fully polarized along the z axis. (b) Decreasing the frequency, the optical magnon BEC transition is provoked on the point $\tilde{\Omega} = \tilde{\Omega}_{\text{BEC}}$, where the AF acquires a transverse component of local magnetization associated with the spontaneous $U(1)$ symmetry breaking. Thus a macroscopic coherent state is formed. (c) In the low frequency regime $\tilde{\Omega} \sim 0$, the Néel magnetic order is developed on the xy plane and we take it the x axis without loss of generality. Throughout this paper we study the optical magnon BEC (b) in the vicinity of $\tilde{\Omega} = \tilde{\Omega}_{\text{BEC}}$.

APPENDIX B: MAGNON THEORY

In this Appendix we derive the transition point for the magnon BEC, Ω_{BEC} , associated with the fully spin-polarized state in the high frequency regime, and evaluate the number of magnon condensates in the vicinity of $\Omega = \Omega_{\text{BEC}}$. The ground state is fully polarized $\mathbf{S} = (0, 0, \eta S)$ for $\Omega > \Omega_c$. First, we perform the Holstein-Primakoff transformation,

$$\begin{aligned}\eta \hat{S}_i^z &= S - \hat{n}_i, \\ \hat{S}_i^x + \eta i \hat{S}_i^y &= \sqrt{2S} \left(1 - \frac{\hat{n}_i}{2S}\right)^{1/2} \hat{a}_i, \\ \hat{S}_i^x - \eta i \hat{S}_i^y &= \sqrt{2S} \hat{a}_i^\dagger \left(1 - \frac{\hat{n}_i}{2S}\right)^{1/2},\end{aligned}$$

where \hat{a}_i^\dagger and \hat{a}_i are creation and annihilation operators for bosons, i.e., magnons, and $\hat{n}_i \equiv \hat{a}_i^\dagger \hat{a}_i$ is the number operator. We make an expansion and retain up to the fourth order terms of \hat{a}_i and \hat{a}_i^\dagger ,

$$\begin{aligned}\eta \hat{S}_i^z &= S - \hat{n}_i, \\ \hat{S}_i^x + \eta i \hat{S}_i^y &= \sqrt{2S} \left(1 - \frac{\hat{n}_i}{4S}\right) \hat{a}_i, \\ \hat{S}_i^x - \eta i \hat{S}_i^y &= \sqrt{2S} \hat{a}_i^\dagger \left(1 - \frac{\hat{n}_i}{4S}\right).\end{aligned}$$

$$\begin{aligned}\hat{U} &= -\frac{J}{2N} \sum_{\mathbf{k}_1, \mathbf{k}_2, \mathbf{k}_3, \mathbf{k}_4} [\cos(k_{1,x}a) + \cos(k_{1,y}a) + \cos(k_{1,z}a)] \hat{a}_{\mathbf{k}_1}^\dagger \hat{a}_{\mathbf{k}_2}^\dagger \hat{a}_{\mathbf{k}_3} \hat{a}_{\mathbf{k}_4} \delta_{\mathbf{k}_1 + \mathbf{k}_2, \mathbf{k}_3 + \mathbf{k}_4} \\ &\quad - \frac{J}{2N} \sum_{\mathbf{k}_1, \mathbf{k}_2, \mathbf{k}_3, \mathbf{k}_4} [\cos(k_{4,x}a) + \cos(k_{4,y}a) + \cos(k_{4,z}a)] \hat{a}_{\mathbf{k}_1}^\dagger \hat{a}_{\mathbf{k}_2}^\dagger \hat{a}_{\mathbf{k}_3} \hat{a}_{\mathbf{k}_4} \delta_{\mathbf{k}_1 + \mathbf{k}_2, \mathbf{k}_3 + \mathbf{k}_4} \\ &\quad + \frac{J}{N} \sum_{\mathbf{k}_1, \mathbf{k}_2, \mathbf{k}_3, \mathbf{k}_4} \{\cos[(k_{1,x} - k_{2,x})a] + \cos[(k_{1,y} - k_{2,y})a] + \cos[(k_{1,z} - k_{2,z})a]\} \hat{a}_{\mathbf{k}_1}^\dagger \hat{a}_{\mathbf{k}_2} \hat{a}_{\mathbf{k}_3}^\dagger \hat{a}_{\mathbf{k}_4} \delta_{\mathbf{k}_1 + \mathbf{k}_3, \mathbf{k}_2 + \mathbf{k}_4} \\ &\quad + \frac{D}{N} \sum_{\mathbf{k}_1, \mathbf{k}_2, \mathbf{k}_3, \mathbf{k}_4} \hat{a}_{\mathbf{k}_1}^\dagger \hat{a}_{\mathbf{k}_2} \hat{a}_{\mathbf{k}_3}^\dagger \hat{a}_{\mathbf{k}_4} \delta_{\mathbf{k}_1 + \mathbf{k}_3, \mathbf{k}_2 + \mathbf{k}_4}.\end{aligned}\tag{B3}$$

The magnon Hamiltonian in the corotating frame [Eq. (B2)] consists of the kinetic energy, the magnon-magnon interaction, and the Zeeman energy of the magnetic field in the magnet. The effective magnetic field $\mathbf{B}_{\text{eff}} = (B_{\text{eff}}^x, 0, B_{\text{eff}}^z)$ magnons acquired in the corotating frame is $B_{\text{eff}}^z := \hbar(\Omega - \Omega_{\text{BEC}}) + 6JS$ along the z axis, while $B_{\text{eff}}^x := B_0$ along the x axis. Since $6JS = O(10)$ meV $\sim O(10^2)$ T and consequently $6JS \gg B_0$ in general, the effective magnetic field along the x axis $B_{\text{eff}}^x = B_0$ is negligibly small compared with the z component $B_{\text{eff}}^z \ll B_{\text{eff}}^z$ even in the vicinity of $\Omega \approx \Omega_{\text{BEC}}$. When Ω is decreased from the large value, the band $2JS[\cos(k_x a) + \cos(k_y a) + \cos(k_z a)] - z_0 JS - 2DS + \hbar\Omega$ touches the zero energy at the wave number $\mathbf{k} = \boldsymbol{\pi} := (\pi/a, \pi/a, \pi/a)$. Therefore the magnons created by \hat{a}_π^\dagger condensate at

$$\hbar\Omega_{\text{BEC}} = 2(6J + D)S,\tag{B4}$$

which coincides with $\hbar\Omega_c$ [Eq. (A6)].

Using the magnon operator, the Hamiltonian [Eq. (A2)] is rewritten as

$$\begin{aligned}\hat{\mathcal{H}}_{\text{eff}} &= JS \sum_{(i,j)} (\hat{a}_i^\dagger \hat{a}_j + \text{H.c.}) - \frac{J}{4} \sum_{(i,j)} (\hat{a}_i^\dagger \hat{n}_i \hat{a}_j + \hat{a}_i^\dagger \hat{n}_j \hat{a}_j + \text{H.c.}) \\ &\quad - z_0 JS \sum_i \hat{n}_i + J \sum_{(i,j)} \hat{n}_i \hat{n}_j - 2DS \sum_i \hat{n}_i + D \sum_i \hat{n}_i^2 \\ &\quad + \hbar\Omega \sum_i \hat{n}_i,\end{aligned}\tag{B1}$$

where constant terms are dropped. We consider the cubic lattice and the configuration number is $z_0 = 6$. After the Fourier transform for the positional vector \mathbf{r}_i as

$$\hat{a}_\mathbf{k} = \sqrt{\frac{1}{N}} \sum_i e^{-i\mathbf{k}\cdot\mathbf{r}_i} \hat{a}_i, \quad \hat{a}_\mathbf{k}^\dagger = \sqrt{\frac{1}{N}} \sum_i e^{i\mathbf{k}\cdot\mathbf{r}_i} \hat{a}_i^\dagger, \quad \hat{n}_\mathbf{k} = \hat{a}_\mathbf{k}^\dagger \hat{a}_\mathbf{k},$$

we obtain

$$\begin{aligned}\hat{\mathcal{H}}_{\text{eff}} &= 2JS \sum_{\mathbf{k}} [\cos(k_x a) + \cos(k_y a) + \cos(k_z a)] \hat{n}_\mathbf{k} \\ &\quad + (-z_0 JS - 2DS + \hbar\Omega) \sum_{\mathbf{k}} \hat{n}_\mathbf{k} + \hat{U},\end{aligned}\tag{B2}$$

where a is the lattice constant. The interaction term \hat{U} is represented as

Next, we consider the interaction term. Since magnons condensate at $\mathbf{k} = \boldsymbol{\pi}$, we only keep the term with $\mathbf{k}_1 = \mathbf{k}_2 = \mathbf{k}_3 = \mathbf{k}_4 = \boldsymbol{\pi}$ in Eq. (B3) as

$$\hat{U} = \frac{3J}{N} \hat{a}_\pi^\dagger \hat{a}_\pi^\dagger \hat{a}_\pi \hat{a}_\pi + \frac{3J + D}{N} \hat{a}_\pi^\dagger \hat{a}_\pi \hat{a}_\pi^\dagger \hat{a}_\pi\tag{B5a}$$

$$= \frac{6J + D}{N} \hat{a}_\pi^\dagger \hat{a}_\pi^\dagger \hat{a}_\pi \hat{a}_\pi + \frac{3J + D}{N} \hat{n}_\pi.\tag{B5b}$$

Thus $6J + D > 0$ corresponds to repulsive interaction. The $\mathbf{k} = \boldsymbol{\pi}$ sector in the Hamiltonian of Eq. (B2) is given as

$$\begin{aligned}\hat{\mathcal{H}}_{\text{eff}}(\mathbf{k} = \boldsymbol{\pi}) &= \left(-12JS - 2DS + \hbar\Omega + \frac{3J + D}{N}\right) \hat{n}_\pi \\ &\quad + \frac{6J + D}{N} \hat{a}_\pi^\dagger \hat{a}_\pi^\dagger \hat{a}_\pi \hat{a}_\pi.\end{aligned}\tag{B6}$$

Since we treat a macroscopic system, the number of spin sites N is large enough to approximate as

$$\hat{\mathcal{H}}_{\text{eff}}(\mathbf{k} = \boldsymbol{\pi}) \simeq (-12JS - 2DS + \hbar\Omega)\hat{n}_{\boldsymbol{\pi}} + \frac{6J + D}{N}\hat{a}_{\boldsymbol{\pi}}^{\dagger}\hat{a}_{\boldsymbol{\pi}}^{\dagger}\hat{a}_{\boldsymbol{\pi}}\hat{a}_{\boldsymbol{\pi}} \quad (\text{B7a})$$

$$= \hbar(\Omega - \Omega_{\text{BEC}})\hat{n}_{\boldsymbol{\pi}} + \frac{\hbar\Omega_{\text{BEC}}}{2NS}\hat{a}_{\boldsymbol{\pi}}^{\dagger}\hat{a}_{\boldsymbol{\pi}}^{\dagger}\hat{a}_{\boldsymbol{\pi}}\hat{a}_{\boldsymbol{\pi}}. \quad (\text{B7b})$$

In order for the magnon BEC state with finite $\langle \hat{n}_{\boldsymbol{\pi}} \rangle$ to be stabilized, the repulsive interaction $6J + D > 0$ is necessary, which corresponds to Eq. (A5).

Finally, by minimizing Eq. (B7a) we obtain

$$\langle \hat{n}_{\boldsymbol{\pi}} \rangle = \frac{12JS + 2DS - \hbar\Omega}{2(6J + D)}N \quad (\text{B8a})$$

$$= \frac{\Omega_{\text{BEC}} - \Omega}{\Omega_{\text{BEC}}}NS. \quad (\text{B8b})$$

Thus the number of magnon condensates is characterized as a function of laser frequency Ω for $\Omega < \Omega_{\text{BEC}}$. The magnetization along the z axis per spin is provided as

$$\frac{\langle \eta \sum_i \hat{S}_i^z \rangle}{N} = S - \frac{\langle \sum_i \hat{n}_i \rangle}{N} \quad (\text{B9a})$$

$$\simeq S - \frac{\langle \hat{n}_{\boldsymbol{\pi}} \rangle}{N} \quad (\text{B9b})$$

$$= \frac{\Omega}{\Omega_{\text{BEC}}}S, \quad (\text{B9c})$$

which corresponds to Eq. (A7c).

APPENDIX C: REFERENCE FRAME

In this Appendix we give the description in the original stationary reference frame. Note that in Appendices A and B we describe the system in the rotating frame. We represent the transformation $R := \exp(\eta i\Omega t S^z)$ to the rotating frame. The observables transform as

$$\begin{aligned} (\tilde{S}^x, \tilde{S}^y) &= R^{-1}(S^x, S^y)R \\ &= [\cos(\Omega t)S^x + \eta \sin(\Omega t)S^y, -\eta \sin(\Omega t)S^x \\ &\quad + \cos(\Omega t)S^y]. \end{aligned}$$

The Heisenberg equation of motion is as

$$\begin{aligned} i\partial_t \tilde{\mathcal{O}} &= i\partial_t (R^{\dagger} \mathcal{O} R) \\ &= (i\partial_t R^{\dagger}) \mathcal{O} R + R^{\dagger} (i\partial_t \mathcal{O}) R + R^{\dagger} \mathcal{O} (i\partial_t R) \\ &= (i\partial_t R^{\dagger}) R \tilde{\mathcal{O}} + R^{\dagger} [\mathcal{O}, \mathcal{H}] R + \tilde{\mathcal{O}} R^{\dagger} (i\partial_t R) \\ &= [\tilde{\mathcal{O}}, \tilde{\mathcal{H}} + R^{\dagger} (i\partial_t R)]. \end{aligned}$$

Thus the effective Hamiltonian is given as $\tilde{\mathcal{H}} + R^{\dagger} (i\partial_t R) = \tilde{\mathcal{H}} - \eta\Omega S^z$.

The purpose of this Appendix is to give the description in the original stationary reference frame. First, we represent the magnon operators in the reference frame as $\hat{b}_k^{(\dagger)}$, i.e.,

$$\hat{a}_k^{(\dagger)} = \hat{R}^{\dagger} \hat{b}_k^{(\dagger)} \hat{R}, \quad (\text{C1})$$

where $\hat{R} = \exp(\eta i\Omega t \hat{S}_{\text{tot}}^z) = \exp[i\Omega t (NS - \sum_k \hat{a}_k^{\dagger} \hat{a}_k)]$. The time evolution is evaluated as

$$\begin{aligned} i\hbar\partial_t \hat{b}_k^{(\dagger)} &= i\hbar\partial_t (\hat{R} \hat{a}_k^{(\dagger)} \hat{R}^{\dagger}) \\ &= (i\hbar\partial_t \hat{R}) \hat{a}_k^{(\dagger)} \hat{R}^{\dagger} + \hat{R} (i\hbar\partial_t \hat{a}_k^{(\dagger)}) \hat{R}^{\dagger} + \hat{R} \hat{a}_k^{(\dagger)} (i\hbar\partial_t \hat{R}^{\dagger}) \\ &= -\hbar\Omega \hat{R} \left(NS - \sum_k \hat{a}_k^{\dagger} \hat{a}_k \right) \hat{R}^{\dagger} \hat{a}_k^{(\dagger)} \hat{R}^{\dagger} + \hat{R} [\hat{a}_k^{(\dagger)}, \hat{\mathcal{H}}] \hat{R}^{\dagger} + \hbar\Omega \hat{R} \hat{a}_k^{(\dagger)} \hat{R}^{\dagger} \hat{R} \left(NS - \sum_k \hat{a}_k^{\dagger} \hat{a}_k \right) \hat{R}^{\dagger} \\ &= -\hbar\Omega \left(NS - \sum_k \hat{b}_k^{\dagger} \hat{b}_k \right) \hat{b}_k^{(\dagger)} + [\hat{b}_k^{(\dagger)}, \hat{R} \hat{\mathcal{H}} \hat{R}^{\dagger}] + \hbar\Omega \hat{b}_k^{(\dagger)} \left(NS - \sum_k \hat{b}_k^{\dagger} \hat{b}_k \right) \\ &= \left[\hat{b}_k^{(\dagger)}, \hat{R} \hat{\mathcal{H}} \hat{R}^{\dagger} + \hbar\Omega \left(NS - \sum_k \hat{b}_k^{\dagger} \hat{b}_k \right) \right] \\ &= \left[\hat{b}_k^{(\dagger)}, \hat{R} \hat{\mathcal{H}} \hat{R}^{\dagger} - \hbar\Omega \sum_k \hat{b}_k^{\dagger} \hat{b}_k \right]. \end{aligned} \quad (\text{C2})$$

Next, we focus on the $\mathbf{k} = \boldsymbol{\pi}$ sector. The effective Hamiltonian in the rotating frame is given as Eq. (B7b);

$$\hat{\mathcal{H}}_{\text{eff}}(\mathbf{k} = \boldsymbol{\pi}) = \hbar(\Omega - \Omega_{\text{BEC}})\hat{a}_{\boldsymbol{\pi}}^{\dagger}\hat{a}_{\boldsymbol{\pi}} + \frac{\hbar\Omega_{\text{BEC}}}{2NS}\hat{a}_{\boldsymbol{\pi}}^{\dagger}\hat{a}_{\boldsymbol{\pi}}^{\dagger}\hat{a}_{\boldsymbol{\pi}}\hat{a}_{\boldsymbol{\pi}}.$$

Finally, from Eq. (C2) we obtain the corresponding Hamiltonian in the original stationary reference frame as

$$\hat{R} \hat{\mathcal{H}}_{\text{eff}}(\mathbf{k} = \boldsymbol{\pi}) \hat{R}^{\dagger} - \hbar\Omega \hat{b}_{\boldsymbol{\pi}}^{\dagger} \hat{b}_{\boldsymbol{\pi}} = -\hbar\Omega_{\text{BEC}} \hat{b}_{\boldsymbol{\pi}}^{\dagger} \hat{b}_{\boldsymbol{\pi}} + \frac{\hbar\Omega_{\text{BEC}}}{2NS} \hat{b}_{\boldsymbol{\pi}}^{\dagger} \hat{b}_{\boldsymbol{\pi}}^{\dagger} \hat{b}_{\boldsymbol{\pi}} \hat{b}_{\boldsymbol{\pi}} \quad (\text{C3a})$$

$$=: \hat{\mathcal{H}}_{\mathbf{k}=\boldsymbol{\pi}}. \quad (\text{C3b})$$

The equation of motion is given as

$$\begin{aligned} i\hbar\partial_t\hat{b}_\pi &= \left[\hat{b}_\pi, -\hbar\Omega_{\text{BEC}}\hat{b}_\pi^\dagger\hat{b}_\pi + \frac{\hbar\Omega_{\text{BEC}}}{2NS}\hat{b}_\pi^\dagger\hat{b}_\pi^\dagger\hat{b}_\pi\hat{b}_\pi \right] \\ &= -\hbar\Omega_{\text{BEC}}\hat{b}_\pi + \frac{\hbar\Omega_{\text{BEC}}}{NS}\hat{b}_\pi^\dagger\hat{b}_\pi\hat{b}_\pi, \end{aligned} \quad (\text{C4a})$$

$$\begin{aligned} i\hbar\partial_t\hat{b}_\pi^\dagger &= \left[\hat{b}_\pi^\dagger, -\hbar\Omega_{\text{BEC}}\hat{b}_\pi^\dagger\hat{b}_\pi + \frac{\hbar\Omega_{\text{BEC}}}{2NS}\hat{b}_\pi^\dagger\hat{b}_\pi^\dagger\hat{b}_\pi\hat{b}_\pi \right] \\ &= \hbar\Omega_{\text{BEC}}\hat{b}_\pi^\dagger - \frac{\hbar\Omega_{\text{BEC}}}{NS}\hat{b}_\pi^\dagger\hat{b}_\pi^\dagger\hat{b}_\pi. \end{aligned} \quad (\text{C4b})$$

If we approximate $\hat{b}_\pi^\dagger\hat{b}_\pi = \hat{a}_\pi^\dagger\hat{a}_\pi \simeq [(\Omega_{\text{BEC}} - \Omega)/\Omega_{\text{BEC}}]NS$, cf., Eq. (B8b), those reduce to

$$i\hbar\partial_t\hat{b}_\pi = -\hbar\Omega\hat{b}_\pi, \quad i\hbar\partial_t\hat{b}_\pi^\dagger = \hbar\Omega\hat{b}_\pi^\dagger. \quad (\text{C5})$$

These equations represent the precession with the frequency Ω in synchronization with the laser field.

APPENDIX D: OPTOMAGNONIC JOSEPHSON EQUATION

In this Appendix, starting from the Hamiltonian $\hat{\mathcal{H}}_{\text{tot}} = \hat{\mathcal{H}}_L + \hat{\mathcal{H}}_R + \hat{V}$ for the junction of weakly coupled two magnon BECs (see the main text), we derive the optomagnonic Josephson equations in the main text. First, the Heisenberg equation of motion provides

$$i\hbar\frac{d\hat{b}_L}{dt} = [\hat{b}_L, \hat{\mathcal{H}}_L + \hat{V}] \quad (\text{D1a})$$

$$= \hbar\Omega_L\hat{b}_L + 2U_L\hat{b}_L^\dagger\hat{b}_L\hat{b}_L - K\hat{b}_R^\dagger, \quad (\text{D1b})$$

$$i\hbar\frac{d\hat{b}_R}{dt} = [\hat{b}_R, \hat{\mathcal{H}}_R + \hat{V}] \quad (\text{D1c})$$

$$= \hbar\Omega_R\hat{b}_R + 2U_R\hat{b}_R^\dagger\hat{b}_R\hat{b}_R - K\hat{b}_L^\dagger. \quad (\text{D1d})$$

Taking the expectation value $\langle \hat{b}_{L(R)} \rangle =: b_{L(R)} \in \mathbb{C}$, we obtain the two-state model in the main text.

Next, noting that $(db_{L(R)}/dt)/b_{L(R)} = (d/dt)\ln b_{L(R)}$ and multiplying the two-state model by $1/b_{L(R)}$, it is recast into

$$i\hbar\frac{d}{dt}\ln b_L = \hbar\Omega_L + 2U_LN_L - K\frac{b_R^\dagger}{b_L}, \quad (\text{D2a})$$

$$i\hbar\frac{d}{dt}\ln b_R = \hbar\Omega_R + 2U_RN_R - K\frac{b_L^\dagger}{b_R}. \quad (\text{D2b})$$

Since $b_L(t) = \sqrt{N_L(t)}e^{i\theta_L(t)}$ and $b_R(t) = \sqrt{N_R(t)}e^{-i\theta_R(t)}$, those are rewritten as

$$i\hbar\left(\frac{1}{2}\frac{1}{N_L}\frac{dN_L}{dt} + i\frac{d\theta_L}{dt}\right) = \hbar\Omega_L + 2U_LN_L - K\sqrt{\frac{N_R}{N_L}}e^{i(\theta_R - \theta_L)}, \quad (\text{D3a})$$

$$i\hbar\left(\frac{1}{2}\frac{1}{N_R}\frac{dN_R}{dt} - i\frac{d\theta_R}{dt}\right) = \hbar\Omega_R + 2U_RN_R - K\sqrt{\frac{N_L}{N_R}}e^{i(\theta_R - \theta_L)}. \quad (\text{D3b})$$

Dividing Eq. (D3a) into the real and imaginary parts, we obtain

$$-\hbar\frac{d\theta_L}{dt} = (\hbar\Omega_L + 2U_LN_L) - K\sqrt{\frac{N_R}{N_L}}\cos(\theta_R - \theta_L), \quad (\text{D4a})$$

$$\hbar\frac{dN_L}{dt} = -2K\sqrt{N_LN_R}\sin(\theta_R - \theta_L). \quad (\text{D4b})$$

In the same way, Eq. (D3b) provides

$$\hbar\frac{d\theta_R}{dt} = (\hbar\Omega_R + 2U_RN_R) - K\sqrt{\frac{N_L}{N_R}}\cos(\theta_R - \theta_L), \quad (\text{D5a})$$

$$\hbar\frac{dN_R}{dt} = -2K\sqrt{N_LN_R}\sin(\theta_R - \theta_L). \quad (\text{D5b})$$

Here we remark that the calculation of Eq. (D4b) – Eq. (D5b) gives

$$\frac{d}{dt}(N_L - N_R) = 0. \quad (\text{D6})$$

This means that the total spin angular momentum is conserved and $N_- := N_L - N_R$ is constant. On the other hand, the calculation of Eq. (D4b) + Eq. (D5b) provides

$$\frac{d}{dt}(N_L + N_R) = -\frac{4K}{\hbar}\sqrt{N_LN_R}\sin(\theta_R - \theta_L). \quad (\text{D7})$$

This describes the magnonic Josephson spin current flowing across the junction interface. Introducing $N_+(t) := N_L(t) + N_R(t) > 0$ and defining $z(t) := N_+(t)/N_-$, it satisfies

$$|z(t)| \geq 1. \quad (\text{D8})$$

In this work, without loss of generality, we assume the initial condition $N_-(0) > 0$ for convenience. Since $N_- := N_L - N_R$ is constant, this ensures $z(t) \geq 1$ and

$$z^2 = \frac{N_-^2 + 4N_LN_R}{N_-^2} \quad (\text{D9a})$$

$$= 1 + 4\frac{N_LN_R}{N_-^2}, \quad (\text{D9b})$$

resulting in

$$\frac{\sqrt{N_LN_R}}{N_-} = \frac{\sqrt{z^2 - 1}}{2}. \quad (\text{D10})$$

Finally, using the relation, from Eq. (D7) we obtain

$$\frac{dz(t)}{dt} = -\frac{2K}{\hbar}\sqrt{z(t)^2 - 1}\sin\theta(t), \quad (\text{D11})$$

where $\theta(t) := \theta_R(t) - \theta_L(t)$ is the relative phase. The calculation of Eq. (D4a) + Eq. (D5a) gives

$$\begin{aligned} \hbar\frac{d}{dt}(\theta_R - \theta_L) &= (\hbar\Omega_L + \hbar\Omega_R) + 2(U_LN_L + U_RN_R) \\ &\quad - K\left(\sqrt{\frac{N_R}{N_L}} + \sqrt{\frac{N_L}{N_R}}\right)\cos(\theta_R - \theta_L). \end{aligned} \quad (\text{D12})$$

Since

$$\sqrt{\frac{N_R}{N_L}} + \sqrt{\frac{N_L}{N_R}} = \frac{2}{\sqrt{z^2 - 1}} z, \quad (\text{D13a})$$

$$U_L N_L + U_R N_R = \frac{U_L + U_R}{2} N_{-z} + \frac{U_L - U_R}{2} N_{-}, \quad (\text{D13b})$$

Eq. (D12) is rewritten as

$$\begin{aligned} \frac{d\theta(t)}{dt} = & \left[(\Omega_L + \Omega_R) + \frac{U_L - U_R}{\hbar} N_{-} \right] + \left(\frac{U_L + U_R}{\hbar} N_{-} \right) z(t) \\ & - \frac{2K}{\hbar} \frac{z(t)}{\sqrt{z(t)^2 - 1}} \cos\theta(t). \end{aligned} \quad (\text{D14})$$

Equations (D11) and (D14) are the optomagnonic Josephson equation in the main text.

We remark that introducing the normalized time

$$\tau := \frac{2K}{\hbar} t, \quad (\text{D15})$$

the optomagnonic Josephson equations [Eqs. (D11) and (D14)] are recast into the dimensionless form as

$$\frac{dz(\tau)}{d\tau} = -\sqrt{z(\tau)^2 - 1} \sin\theta(\tau), \quad (\text{D16a})$$

$$\begin{aligned} \frac{d\theta(\tau)}{d\tau} = & \left[\frac{\hbar(\Omega_L + \Omega_R)}{2K} + \frac{U_L - U_R}{2K} N_{-} \right] \\ & + \left(\frac{U_L + U_R}{2K} N_{-} \right) z(\tau) - \frac{z(\tau)}{\sqrt{z(\tau)^2 - 1}} \cos\theta(\tau). \end{aligned} \quad (\text{D16b})$$

APPENDIX E: TUNNELING AMPLITUDE

In this Appendix we estimate the tunneling amplitude in spin language. Due to a finite overlap of the wave functions of the localized spins that reside on the relevant two-dimensional boundaries of each insulator, there exists in general a finite exchange interaction between the boundary spins. Let us assume that it is described by the boundary spin Hamiltonian

as $\hat{V}_s = -J_{\text{tun}} \hat{S}_L \cdot \hat{S}_R$, where $\hat{S}_{L(R)}$ is the spin operator for the boundary spins forming the macroscopic coherent state; the spin quantum number in the left (right) insulator is $S_{L(R)}$ and J_{tun} of $|J_{\text{tun}}| \ll J$ is the weak spin exchange interaction between the boundary spins. By means of the magnon theory, it reduces to the tunneling Hamiltonian \hat{V} in the main text as $\hat{V}_s \approx -J_{\text{tun}} \sqrt{S_L S_R} (\hat{b}_L \hat{b}_R + \hat{b}_L^\dagger \hat{b}_R^\dagger)$. Thus we find that the tunneling amplitude is represented in spin language as

$$|K| = |J_{\text{tun}}| \sqrt{S_L S_R}. \quad (\text{E1})$$

Note that $\text{sgn}(K) = \text{sgn}(J_{\text{tun}}) = \pm$ in general, see the main text.

APPENDIX F: AN ANALYSIS ON OPTOMAGNOMIC DC JOSEPHSON EFFECT

In this Appendix under the assumption that magnon BECs are realized stably, we discuss an attempt to realize an optomagnonic DC Josephson effect. Assuming the initial condition $z(0) \gg 1$ and tuning the parameters as $\hbar(\Omega_L + \Omega_R) + (U_L - U_R) N_{-} = 0$ and $U_L + U_R = 0$, the optomagnonic Josephson equation in the main text is recast into

$$\left. \frac{dz(\tau)}{d\tau} \right|_{\tau \ll 1} = -z(\tau) \sin\theta(\tau), \quad (\text{F1a})$$

$$\left. \frac{d\theta(\tau)}{d\tau} \right|_{\tau \ll 1} = -\cos\theta(\tau), \quad (\text{F1b})$$

where $\tau := (2K/\hbar)t$ is the normalized time. Noting that $d\theta(\tau)/(d\tau)|_{\tau \ll 1} = 0$ when $\theta(0) = \pm\pi/2$, we find that the functions, $z(\tau)|_{\tau \ll 1} = -z(0)\tau + z(0)$ and $z(\tau)|_{\tau \ll 1} = z(0)\tau + z(0)$, approximately satisfy the Josephson equation for $\theta(0) = \pi/2$ and $\theta(0) = -\pi/2$, respectively. This implies that the DC Josephson effect satisfying $dz(\tau)/(d\tau)|_{\tau \ll 1} = (\text{const.})$ and $d\theta(\tau)/(d\tau)|_{\tau \ll 1} = 0$ is induced for $\tau \ll 1$.

From this, one might suspect that the DC Josephson effect is realizable. However, it requires the condition $U_L + U_R = 0$, which means that the magnon-magnon interaction is attractive on one side. Therefore, the magnon BEC state itself is unstable on one side as long as one employs this setup.

-
- [1] A. V. Chumak, V. I. Vasyuchka, A. A. Serga, and B. Hillebrands, *Nat. Phys.* **11**, 453 (2015).
 [2] K. Nakata, P. Simon, and D. Loss, *J. Phys. D: Appl. Phys.* **50**, 114004 (2017).
 [3] T. Oka and S. Kitamura, *Annu. Rev. Condens. Matter Phys.* **10**, 387 (2019).
 [4] H. Katsura, N. Nagaosa, and A. V. Balatsky, *Phys. Rev. Lett.* **95**, 057205 (2005).
 [5] M. Sato, S. Takayoshi, and T. Oka, *Phys. Rev. Lett.* **117**, 147202 (2016).
 [6] H. Ishizuka and M. Sato, *Phys. Rev. Lett.* **122**, 197702 (2019).
 [7] H. Ishizuka and M. Sato, *Phys. Rev. B* **100**, 224411 (2019).
 [8] E. V. Gomonaya and V. M. Loktev, *Low Temp. Phys.* **40**, 17 (2014).
 [9] T. Jungwirth, X. Marti, P. Wadley, and J. Wunderlich, *Nat. Nanotechnol.* **11**, 231 (2016).
 [10] V. Baltz, A. Manchon, M. Tsoi, T. Moriyama, T. Ono, and Y. Tserkovnyak, *Rev. Mod. Phys.* **90**, 015005 (2018).
 [11] P. Němec, M. Fiebig, T. Kampfrath, and A. V. Kimel, *Nat. Phys.* **14**, 229 (2018).
 [12] T. Moriyama, K. Hayashi, K. Yamada, M. Shima, Y. Ohya, Y. Tserkovnyak, and T. Ono, *Phys. Rev. B* **101**, 060402(R) (2020).
 [13] J. Li, C. B. Wilson, R. Cheng, M. Lohmann, M. Kavand, W. Yuan, M. Aldosary, N. Agladze, P. Wei, M. S. Sherwin, and J. Shi, *Nature (London)* **578**, 70 (2020).
 [14] P. Vaidya, S. A. Morley, J. van Tol, Y. Liu, R. Cheng, A. Brataas, D. Lederman, and E. del Barco, *Science* **368**, 160 (2020).
 [15] R. Cheng, J. Xiao, Q. Niu, and A. Brataas, *Phys. Rev. Lett.* **113**, 057601 (2014).
 [16] R. Cheng, D. Xiao, and A. Brataas, *Phys. Rev. Lett.* **116**, 207603 (2016).

- [17] S. O. Demokritov, V. E. Demidov, O. Dzyapko, G. A. Melkov, A. A. Serga, B. Hillebrands, and A. N. Slavin, *Nature (London)* **443**, 430 (2006).
- [18] R. Shindou, R. Matsumoto, S. Murakami, and J. I. Ohe, *Phys. Rev. B* **87**, 174427 (2013).
- [19] R. Shindou, J. I. Ohe, R. Matsumoto, S. Murakami, and E. Saitoh, *Phys. Rev. B* **87**, 174402 (2013).
- [20] R. E. Troncoso and A. S. Nunez, *Ann. Phys.* **346**, 182 (2014).
- [21] The analogy of the magnetically ordered state to the superconducting state, i.e., Josephson effect [78], was explained in Ref. [4].
- [22] K. Nakata, K. A. van Hoogdalem, P. Simon, and D. Loss, *Phys. Rev. B* **90**, 144419 (2014).
- [23] See Ref. [79] for thermomagnetic transport of noncoherent magnons associated with the Néel magnetic order in the bulk of insulating AFs.
- [24] Y. Liu, G. Yin, J. Zang, R. K. Lake, and Y. Barlas, *Phys. Rev. B* **94**, 094434 (2016).
- [25] R. Khymyn, I. Lisenkov, V. Tiberkevich, B. A. Ivanov, and A. Slavin, *Sci. Rep.* **7**, 43705 (2017).
- [26] Y. Mukai, H. Hirori, T. Yamamoto, H. Kageyama, and K. Tanaka, *Appl. Phys. Lett.* **105**, 022410 (2014).
- [27] D. Bossini, V. I. Belotelov, A. K. Zvezdin, A. N. Kalish, and A. V. Kimel, *ACS Photon.* **3**, 1385 (2016).
- [28] M. F. Ciappina, J. A. P.-Hernandez, A. S. Landsman, W. A. Okell, S. Zherebtsov, B. Forg, J. Schotz, L. Seiffert, T. Fennel, T. Shaaran, T. Zimmermann, A. Chacon, R. Guichard, A. Zair, J. W. G. Tisch, J. P. Marangos, T. Witting, A. Braun, S. A. Maier, L. Roso *et al.*, *Rep. Prog. Phys.* **80**, 054401 (2017).
- [29] T. Arikawa, S. Morimoto, and K. Tanaka, *Opt. Express* **25**, 13728 (2017).
- [30] A. Kirilyuk, A. V. Kimel, and T. Rasing, *Rev. Mod. Phys.* **82**, 2731 (2010).
- [31] A. V. Kimel, A. Kirilyuk, A. Tsvetkov, R. V. Pisarev, and T. Rasing, *Nature (London)* **429**, 850 (2004).
- [32] A. V. Kimel, A. Kirilyuk, P. A. Usachev, R. V. Pisarev, A. M. Balbashov, and T. Rasing, *Nature (London)* **435**, 655 (2005).
- [33] F. Hansteen, A. Kimel, A. Kirilyuk, and T. Rasing, *Phys. Rev. Lett.* **95**, 047402 (2005).
- [34] C. D. Stanciu, F. Hansteen, A. V. Kimel, A. Tsukamoto, A. Itoh, A. Kirilyuk, and T. Rasing, *Phys. Rev. Lett.* **98**, 207401 (2007).
- [35] A. Rebei and J. Hohlfield, *Phys. Lett. A* **372**, 1915 (2008).
- [36] A. Rebei and J. Hohlfield, *J. Appl. Phys.* **103**, 07B118 (2008).
- [37] C. D. Stanciu, F. Hansteen, A. V. Kimel, A. Kirilyuk, A. Tsukamoto, A. Itoh, and T. Rasing, *Phys. Rev. Lett.* **99**, 047601 (2007).
- [38] I. Radu, K. Vahaplar, C. Stamm, T. Kachel, N. Pontius, H. A. Dürr, T. A. Ostler, J. Barker, R. F. L. Evans, R. W. Chantrell, A. Tsukamoto, A. Itoh, A. Kirilyuk, T. Rasing, and A. V. Kimel, *Nature (London)* **472**, 205 (2011).
- [39] T. A. Ostler, J. Barker, R. F. L. Evans, R. W. Chantrell, U. Atxitia, O. C.-Fesenko, S. E. Moussaoui, L. L. Guyader, E. Mengotti, L. J. Heyderman, F. Nolting, A. Tsukamoto, A. Itoh, D. Afanasiev, B. A. Ivanov, A. M. Kalashnikova, K. Vahaplar, J. Mentink, A. Kirilyuk, T. Rasing *et al.*, *Nat. Commun.* **3**, 666 (2012).
- [40] K. Vahaplar, A. M. Kalashnikova, A. V. Kimel, D. Hinzke, U. Nowak, R. Chantrell, A. Tsukamoto, A. Itoh, A. Kirilyuk, and T. Rasing, *Phys. Rev. Lett.* **103**, 117201 (2009).
- [41] S. J. Barnett, *Phys. Rev.* **6**, 239 (1915).
- [42] S. J. Barnett, *Rev. Mod. Phys.* **7**, 129 (1935).
- [43] M. Matsuo, E. Saitoh, and S. Maekawa, *J. Phys. Soc. Jpn.* **86**, 011011 (2017).
- [44] S. Takayoshi, M. Sato, and T. Oka, *Phys. Rev. B* **90**, 214413 (2014).
- [45] S. Takayoshi, H. Aoki, and T. Oka, *Phys. Rev. B* **90**, 085150 (2014).
- [46] See Refs. [52,53,80–82] for magnon BEC.
- [47] K. Nakata and S. Takayoshi, *Phys. Rev. B* **102**, 094417 (2020).
- [48] A. Osada, R. Hisatomi, A. Noguchi, Y. Tabuchi, R. Yamazaki, K. Usami, M. Sadgrove, R. Yalla, M. Nomura, and Y. Nakamura, *Phys. Rev. Lett.* **116**, 223601 (2016).
- [49] T. Liu, X. Zhang, H. X. Tang, and M. E. Flatté, *Phys. Rev. B* **94**, 060405(R) (2016).
- [50] S. Viola Kusminskiy, H. X. Tang, and F. Marquardt, *Phys. Rev. A* **94**, 033821 (2016).
- [51] See the Appendices for details.
- [52] T. Nikuni, M. Oshikawa, A. Oosawa, and H. Tanaka, *Phys. Rev. Lett.* **84**, 5868 (2000).
- [53] Y. M. Bunkov and G. E. Volovik, *Novel Superfluids*, edited by K. H. Bennemann and J. B. Ketterson (Oxford University Press, Oxford, 2013), Chap IV.
- [54] See also Ref. [47] for the difference from the inverse Faraday effect [30,32].
- [55] M. Sato, T. Higuchi, N. Kanda, K. Konishi, K. Yoshioka, T. Suzuki, K. Misawa, and M. K.-Gonokami, *Nat. Photon.* **7**, 724 (2013).
- [56] S. Kamada, S. Murata, and T. Aoki, *Appl. Phys. Express* **6**, 032701 (2013).
- [57] I. I. Rabi, N. F. Ramsey, and J. Schwinger, *Rev. Mod. Phys.* **26**, 167 (1954).
- [58] T. Holstein and H. Primakoff, *Phys. Rev.* **58**, 1098 (1940).
- [59] K. Nakata, P. Simon, and D. Loss, *Phys. Rev. B* **92**, 134425 (2015).
- [60] P. Bruno, *Phys. Rev. B* **52**, 411 (1995).
- [61] A. Smerzi, S. Fantoni, S. Giovanazzi, and S. R. Shenoy, *Phys. Rev. Lett.* **79**, 4950 (1997).
- [62] Y. Ohnuma, H. Adachi, E. Saitoh, and S. Maekawa, *Phys. Rev. B* **87**, 014423 (2013).
- [63] M. T. Hutchings and E. J. Samuelsen, *Phys. Rev. B* **6**, 3447 (1972).
- [64] E. G. Tveten, A. Qaiumzadeh, and A. Brataas, *Phys. Rev. Lett.* **112**, 147204 (2014).
- [65] M. C. Fischer, J. W. Wilson, F. E. Robles, and W. S. Warren, *Rev. Sci. Instrum.* **87**, 031101 (2016).
- [66] F. Krausz and M. Ivanov, *Rev. Mod. Phys.* **81**, 163 (2009).
- [67] K. Yamaguchi, T. Kurihara, Y. Minami, M. Nakajima, and T. Suemoto, *Phys. Rev. Lett.* **110**, 137204 (2013).
- [68] R. V. Mikhaylovskiy, E. Hendry, V. V. Kruglyak, R. V. Pisarev, T. Rasing, and A. V. Kimel, *Phys. Rev. B* **90**, 184405 (2014).
- [69] D. A. Bozhko, A. A. Serga, P. Clausen, V. I. Vasyuchka, F. Heussner, G. A. Melkov, A. Pomyalov, V. S. L'vov, and B. Hillebrands, *Nat. Phys.* **12**, 1057 (2016).
- [70] S. Autti, P. J. Heikkinen, J. T. Mäkinen, G. E. Volovik, V. V. Zavjalov, and V. B. Eltsov, *Nat. Mater.* **20**, 171 (2021).
- [71] E. Saitoh, M. Ueda, H. Miyajima, and G. Tatara, *Appl. Phys. Lett.* **88**, 182509 (2006).
- [72] A. E. Clark and E. Callen, *J. Appl. Phys.* **39**, 5972 (1968).

- [73] S. Kosen, R. G. E. Morris, A. F. van Loo, and A. D. Karenowska, *Appl. Phys. Lett.* **112**, 012402 (2018).
- [74] Y. Tabuchi, S. Ishino, T. Ishikawa, R. Yamazaki, K. Usami, and Y. Nakamura, *Phys. Rev. Lett.* **113**, 083603 (2014).
- [75] Y. Tabuchi, S. Ichino, A. Noguchi, T. Ishikawa, R. Yamazaki, K. Usami, and Y. Nakamura, *Science* **349**, 405 (2015).
- [76] N. Prasai, B. A. Trump, G. G. Marcus, A. Akopyan, S. X. Huang, T. M. McQueen, and J. L. Cohn, *Phys. Rev. B* **95**, 224407 (2017).
- [77] W. Yuan, Q. Zhu, T. Su, Y. Yao, W. Xing, Y. Chen, Y. Ma, X. Lin, J. Shi, R. Shindou, X. C. Xie, and W. Han, *Sci. Adv.* **4**, eaat1098 (2018).
- [78] B. D. Josephson, *Phys. Lett.* **1**, 251 (1962).
- [79] K. Nakata, S. K. Kim, J. Klinovaja, and D. Loss, *Phys. Rev. B* **96**, 224414 (2017).
- [80] T. Giamarchi, C. Rüegg, and O. Tchernyshyov, *Nat. Phys.* **4**, 198 (2008).
- [81] H. T. Ueda and K. Totsuka, *Phys. Rev. B* **76**, 214428 (2007).
- [82] H. T. Ueda and K. Totsuka, *Phys. Rev. B* **80**, 014417 (2009).